Hypnotic effect of thalidomide is independent of teratogenic ubiquitin/proteasome pathway

Yuki Hirose[a], Tomohiro Kitazono[a], Maiko Sezaki[a], Manabu Abe[b], Kenji Sakimura[b], Hiromasa Funato[a,c], Hiroshi Handa[d], Kaspar E. Vogt[a], and Masashi Yanagisawa[a,e,f,g,1]

[a]International Institute for Integrative Sleep Medicine (WPI-IIIS), University of Tsukuba, Tsukuba, Ibaraki 305-8575, Japan; [b]Department of Cellular Neurobiology, Brain Research Institute, Niigata University, Chuo-ku Niigata 951-8585 Japan; [c]Department of Anatomy, Faculty of Medicine, Toho University, Ota-ku, Tokyo 143-8540, Japan; [d]Department of Chemical Biology, Tokyo Medical University, Shinjuku-ku, Tokyo 160-8402, Japan; [e]Department of Molecular Genetics, University of Texas Southwestern Medical Center, Dallas, TX 75390; [f]Life Science Center for Survival Dynamics, Tsukuba Advanced Research Alliance, University of Tsukuba, 305-8575 Tsukuba, Japan; and [g]R&D Center for Frontiers of MIRAI in Policy and Technology, University of Tsukuba, 305-8575 Tsukuba, Japan

Thalidomide exerts its teratogenic and immunomodulatory effects by binding to cereblon (CRBN) and thereby inhibiting/modifying the CRBN-mediated ubiquitination pathway consisting of the Cullin4-DDB1-ROC1 E3 ligase complex. The mechanism of thalidomide's classical hypnotic effect remains largely unexplored, however. Here we examined whether CRBN is involved in the hypnotic effect of thalidomide by generating mice harboring a thalidomide-resistant mutant allele of *Crbn* (*Crbn YW/AA* knock-in mice). Thalidomide increased non-REM sleep time in *Crbn YW/AA* knock-in homozygotes and heterozygotes to a similar degree as seen in wild-type littermates. Thalidomide similarly depressed excitatory synaptic transmission in the cortical slices obtained from wild-type and *Crbn YW/AA* homozygous knock-in mice without affecting GABAergic inhibition. Thalidomide induced Fos expression in vasopressin-containing neurons of the supraoptic nucleus and reduced Fos expression in the tuberomammillary nuclei. Thus, thalidomide's hypnotic effect seems to share some downstream mechanisms with general anesthetics and GABA$_A$-activating sedatives but does not involve the teratogenic CRBN-mediated ubiquitin/proteasome pathway.

cereblon | sleep | electroencephalography/electromyography (EEG/EMG) | supraoptic nucleus | mouse

Insomnia, a subjective inability to get sufficient sleep (1), is a common complaint in the context of disturbed sleep (2). A variety of GABA$_A$-enhancing hypnotics have been developed and prescribed for patients suffering from insomnia (3). Their side effects include tolerance, addictive potential, motor discoordination, and excessive central nervous system depression that can lead to lethality. In the 1950s, thalidomide was developed as a nonbarbiturate hypnotic agent supposedly with a much better side effect profile. In rodent safety tests, thalidomide showed extremely low acute toxicity with no lethality even at the maximal dose that could be administered orally (5 g/kg) (4). Thalidomide was also commonly taken by pregnant women with morning sickness. Tragically, thalidomide caused severe birth defects in humans, including phocomelia, a dramatic developmental limb malformation (5–9). Thalidomide eluded preclinical toxicologic tests at that time because it does not induce phocomelia or other birth defects in rodents; it is teratogenic only in certain species, including chicken, rabbits, and some primates, including humans (10–12). After the initial market withdrawal, researchers reported clinically favorable effects in patients with erythema nodosum leprosum (13) and HIV infection (14, 15). Thalidomide was also found to have antiangiogenic (16) and immunomodulatory effects (17, 18). Thalidomide and its derivatives have been reintroduced as immunomodulatory drugs to treat certain malignant diseases, especially multiple myeloma, a therapy-resistant neoplastic blood disease (19–21).

Cereblon (CRBN) has been identified as a target molecule for thalidomide-induced teratogenicity (22), and recent reports revealed that CRBN is also the target for thalidomide's therapeutic effect in multiple myeloma (23, 24) and myelodysplastic syndrome with 5q del (25). *Crbn*, originally discovered as a responsible gene for autosomal recessive mild mental retardation in humans (26), encodes one of the substrate receptors forming the Cullin4-DDB1-ROC1 ubiquitin E3 ligase complex. Thalidomide binds human and mouse CRBN with comparable affinity (27), inhibits CRBN autoubiquitination, and can increase CRBN-mediated ubiquitination of other substrates. The thalidomide derivative dBET1, an inhibitor of bromodomain and extraterminal domain protein (BET), binds to mouse and human CRBN at the thalidomide-binding domain (27) and directs E3 ligase activity toward bromodomain-containing 4 (BRD4) (28). Thus, the thalidomide-binding and E3 ligase activities of vertebrate CRBN are conserved, but different substrates are recruited for ubiquitination, resulting in species-specific teratogenic effects (27). Thalidomide-sensitive CRBN signaling, such as regulation of AMP-activated protein kinase activity (29) and of calcium-activated potassium channels (30), has also been reported in mice and rats, respectively.

The mechanism of thalidomide's hypnotic effect is not clear, however. Somers (4) reported that thalidomide did not alter autonomic function or induce respiratory depression or loss of coordination in mice. Kanbayashi et al. (31) reported that thalidomide aggravated symptoms in narcoleptic canines but did not bind or modulate receptors of neurotransmitters that affect sleep/wake, such as orexin, serotonin, histamine, noradrenalin,

Significance

Thalidomide was introduced in 1950s as a safe and effective hypnotic but was subsequently withdrawn from the market due to its devastating teratogenicity in humans. More recently, thalidomide has reemerged as an antineoplastic and immunomodulatory medicine. The teratogenic and immunomodulatory effects of thalidomide have been attributed to direct inhibition of the cereblon-mediated ubiquitin/proteasome pathway. Here we show that cereblon is not involved in the hypnotic effect of thalidomide, using mice that carry a thalidomide-resistant mutant allele of the cereblon gene. Our results suggest the possibility for dissociating the hypnotic effect of thalidomide and its analogs from its teratogenicity.

and GABA. Systematic investigations of thalidomide's actions on brain function are missing.

Protein degradation via the ubiquitin/proteasome pathway could potentially play an important role in the regulation of sleep homeostasis. In forward genetic screening in *Drosophila*, *insomniac* was identified as a responsible gene of a mutant showing severely reduced duration and consolidation of sleep (32). *Insomniac* encodes an adaptor protein, INC, for Cullin3 (CUL3), one of the cullin-family ubiquitin E3 ligases (32, 33). CUL3 interacts with INC and regulates sleep homeostasis (33). This suggests the possibility that a CRBN-containing Cullin complex mediates thalidomide's hypnotic effect. The involvement of CRBN-dependent and -independent signaling pathways is best investigated in a system in which thalidomide can no longer interact with CRBN. A mutated version of human CRBN with amino acid substitutions Y384A and W386A (YW/AA) loses the binding affinity to thalidomide while maintaining the ubiquitin ligase activity. Consequently, *Crbn YW/AA*-mutated chickens and zebrafish are resistant to thalidomide-induced teratogenicity (22).

Here we examined whether the CRBN-mediated ubiquitin/proteasome pathway was involved in the hypnotic effect of thalidomide. To resolve this question, we generated *Crbn YW/AA* knock-in (KI) mice and confirmed that the mutant mouse CRBN is resistant to thalidomide by testing thalidomide-mediated depression of auto-ubiquitination. We recorded electroencephalography/electromyography (EEG/EMG) signals of *Crbn YW/AA* KI mice treated with thalidomide and determined whether thalidomide had a hypnotic effect in these mutants. We also studied the effect of thalidomide on the balance between synaptic excitation and inhibition in the brain, a typical mechanism for a range of hypnotics, and investigated immediate to early gene expression in hypothalamic areas known to be affected by classical sedatives (34).

Results

Hypnotic Effects of Thalidomide in C57BL/6N Mice. The sleep-inducing effect of thalidomide in mice has not been reported in detail. Thalidomide (i.p. at ZT12) increased total non-REM sleep time in a dose-dependent manner and did not reduce total
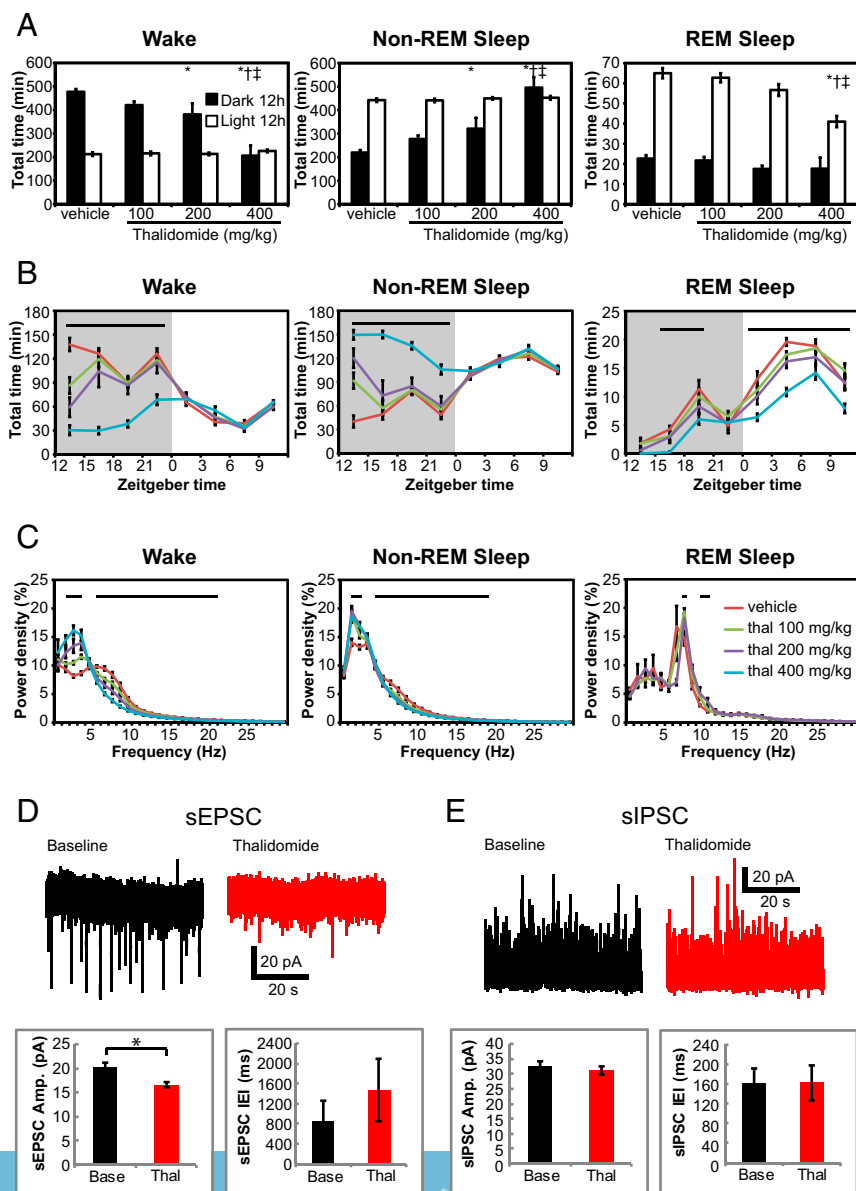
Fig. 1. Hypnotic effect of thalidomide in C57BL/6N mice. C57BL/6N mice were treated with vehicle (0.5% methylcellulose) or thalidomide suspension at dark onset. The EEG/EMG signals were recorded for 24 h after treatment. $n = 8$. Data are mean ± SEM. (*A*) Total time of each state for 24 h after the treatments. *, †,‡ indicate significant difference between object and vehicle, thalidomide 100 mg/kg, and thalidomide 200 mg/kg, respectively. Upper bars indicate significant differences among vehicle and thalidomide 100, 200, and 400 mg/kg ($P < 0.05$). (*B*) The variation of each state per 3 h. (*C*) FFT spectrum analysis of EEG during each state in the 3 h after drug administration. (*D*) Effect of thalidomide (100 μM) on excitatory synaptic transmission. (*Top*) Sample traces from one experiment under baseline conditions (black) and after application of thalidomide (red). (*Bottom*) Summary of the effects on the amplitude (*Left*) and IEI (*Right*) of sEPSCs. (*E*) The effect of thalidomide (100 μM) on inhibitory synaptic transmission. (*Top*) Sample traces under baseline conditions (black) and after application of thalidomide (red). (*Bottom*) Summary of the effects of thalidomide on the amplitude (*Left*) and IEI (*Right*) of sIPSCs.

Hirose et al.

www.manaraa.com

REM sleep time during the 12-h dark phase (Fig. 1*A*). A 400 mg/kg dose of thalidomide reduced total REM sleep time during the subsequent light phase, accompanied by small increases in total wake time and total non-REM sleep time during that period (Fig. 1*A* and *B*).

An analysis of the time spent in each state at 3-h intervals showed that 100 and 200 mg/kg thalidomide increased non-REM sleep time and decreased wake time in the first 3 h, with no significant difference in wake or non-REM sleep time over the next 3 h (Fig. 1*B*). Thus, increased non-REM sleep time during the first 3 h after treatment reflected the initial hypnotic effect of thalidomide. We performed spectral analysis of the EEG in each state during the first 3 h after treatment (Fig. 1*C*). In the wake state, thalidomide dose dependently increased the EEG power density in the 2- to 3-Hz band. Treatment with 100 or 200 mg/kg thalidomide did not alter the EEG power spectrum during REM sleep. No REM sleep state epochs were detected over the 3 h after administration of 400 mg/kg thalidomide. The EEG spectrum during non-REM sleep after thalidomide treatment showed a peak at 2 Hz, corresponding to delta activity. EEG delta power during non-REM sleep after thalidomide treatment was increased compared with that after vehicle treatment (Table 1).

Thalidomide Shifts the Excitation-Inhibition Balance in Mouse Cortex. We tested the effects of thalidomide (100 μM) on neural network activity in mouse cortex by recording spontaneous synaptic activity in acute brain slice preparations in vitro. Thalidomide caused a significant reduction in the amplitude of spontaneous excitatory postsynaptic currents (sEPSCs) ($n = 3$; T = 4.68, $P = 0.043$) and an increase in the interevent interval (IEI) ($n = 3$; T= −2.95, $P = 0.098$)(Fig. 1*D*). There was no significant effect of thalidomide on spontaneous inhibitory synaptic currents (sIPSCs) ($n = 5$; T = 1.16, $P = 0.311$ for amplitude and $n = 5$; T = −0.035, $P = 0.974$ for IEI) (Fig. 1*E*).

Thalidomide Inhibits Autoubiquitination of Mouse CRBN^WT but Not of CRBN^YW/AA. Thalidomide does not cause severe birth defects in rodents including mice (11). This insensitivity to thalidomide-induced malformation in mice could have been due to a resistance of mouse CRBN to thalidomide. Therefore, we verified whether mouse CRBN was inhibited by thalidomide. Mouse CRBN has been demonstrated to bind thalidomide in previous studies (22, 27). Human CRBN forms Cullin4-DDB1-ROC1 ligase complex and is autoubiquitinated when its specific substrates are absent (22). Therefore, we biochemically assessed the extent of autoubiquitination of mouse FLAG-HA–tagged CRBN (FH-CRBN), FH-CRBN^WT, and FH-CRBN^YW/AA. Both FH-CRBN^WT and FH-CRBN^YW/AA were autoubiquitinated in the presence of the proteasome inhibitor MG132 (Fig. 2*B*). Thalidomide attenuated autoubiquitination of FH-CRBN^WT in a concentration-dependent manner, whereas autoubiquitination of FH-CRBN^YW/AA was not affected even at high concentrations of

Table 1. Delta (1 to 6 Hz) and theta (7 to 11 Hz) power as a percentage of total EEG power for increasing doses of thalidomide in WT mice

Dose	Delta power, %	Theta power, %
Vehicle	67.4 ± 1.8	22.6 ± 1.3
Thal 100 mg/kg	73.7 ± 1.3*	17.8 ± 0.8*
Thal 200 mg/kg	76.1 ± 1.5*	15.7 ± 1.2*
Thal 400 mg/kg	77.6 ± 1.3*	14.8 ± 0.9*

Data are mean ± SEM.

*Indicates significant differences from vehicle ($n = 8$; delta power, F = 9.09, $P < 0.001$; theta power, F = 10.52, $P < 0.001$, one-way ANOVA, post hoc comparison to vehicle condition using Tukey's correction).
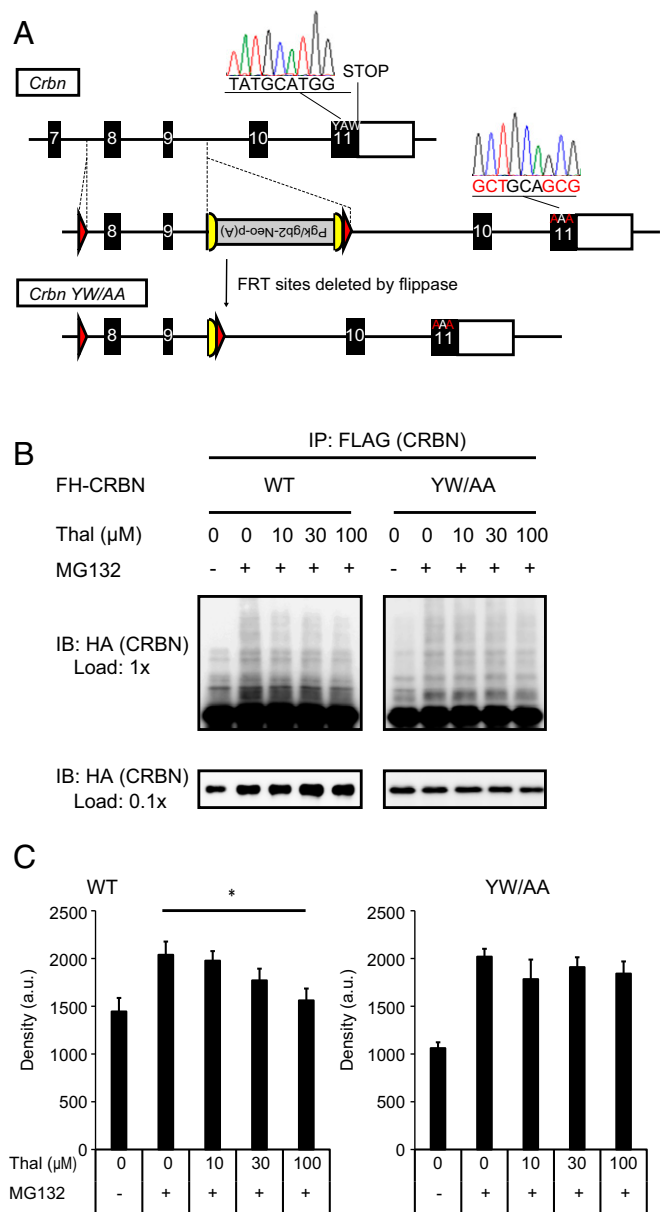
Fig. 2. *Crbn YW/AA* KI mice. (*A*) Generation of *Crbn YW/AA* KI mice. Direct sequencing data at the mutated portion of exon 11 are shown. (*B*) HEK293A cells stably expressing mouse FH-CRBN, FH-CRBN^WT, or FH-CRBN^YW/AA were incubated with the indicated concentrations of thalidomide and MG132. Cell lysates were immunoprecipitated with anti-FLAG antibody and immunoblotted. (*C*) Densitometry quantification of immunoblots in arbitrary units (a.u.). (*Left*) FH-CRBN^WT autoubiquitination is inhibited by thalidomide in a dose-dependent manner ($n = 5$; F = 4.22, $P = 0.03$, one-way repeated-measures ANOVA; *0 μM vs. 100 μM thalidomide, $n = 5$; $P = 0.03$, Bonferroni-corrected, paired Student's *t* test). (*Right*) FH-CRBN^YW/AA autoubiquitination is not affected by thalidomide ($n = 5$; F = 0.83, $P > 0.5$, one-way repeated-measures ANOVA).

thalidomide (Fig. 2 *B* and *C*). Thus, mouse CRBN^YW/AA showed a resistance to thalidomide-induced inhibition of CRBN autoubiquitination, consistent with loss of thalidomide binding (22).

Thalidomide Exerts Similar Hypnotic Effects in *Crbn YW/AA* KI and Wild-Type Mice. We next analyzed whether thalidomide has a hypnotic effect on *Crbn YW/AA* KI mice. There was no significant difference among the genotypes in total time of wake or non-REM sleep in the 12-h dark phase following thalidomide

www.manaraa.com
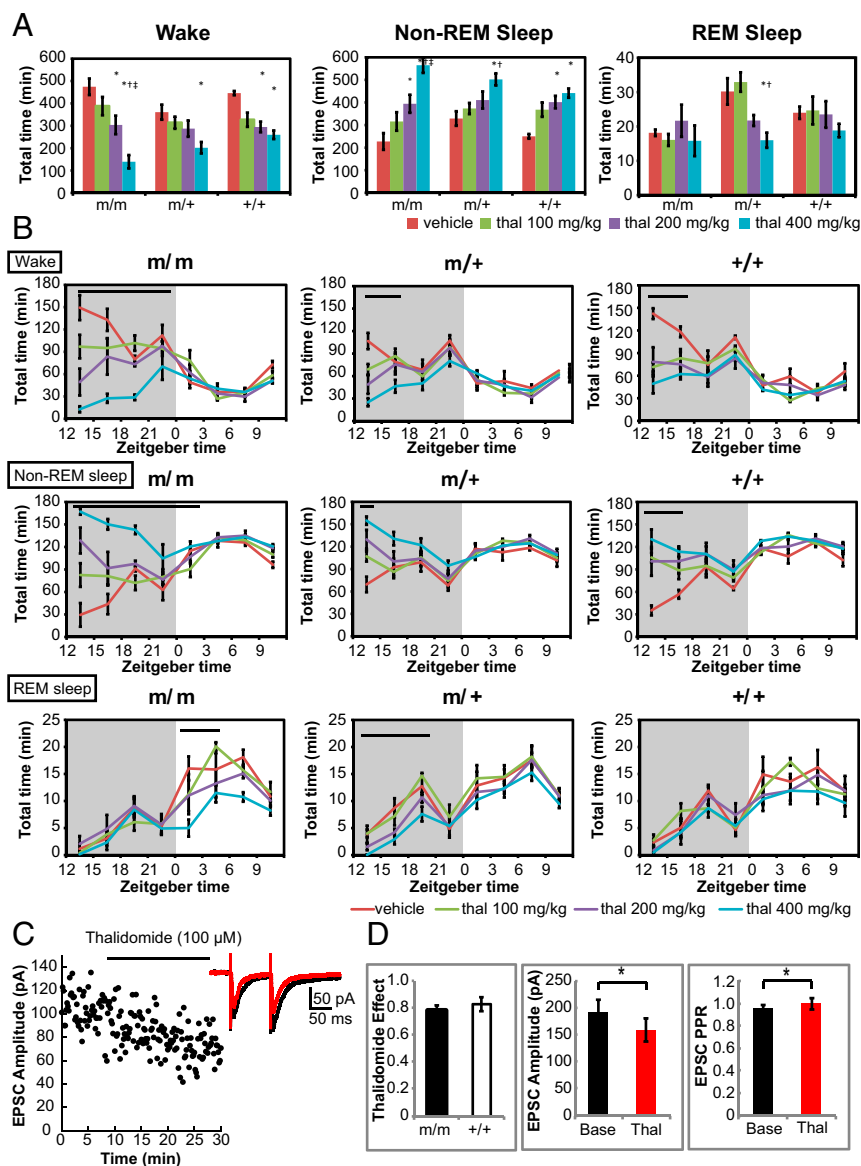
Fig. 3. Hypnotic effect of thalidomide in *Crbn YW/AA* KI mice. *Crbn YW/AA* KI mice were treated with vehicle or thalidomide suspension. The EEG/EMG signals were recorded for 24 h after treatment. m/m, $n = 4$; m/+, $n = 5$; +/+, $n = 4$. Data are mean ± SEM. (*A*) Total time of each state in the 12-h dark period after treatment in each genotype. (*B*) The variation of each state per 3 h. (*C*) Depression of excitatory synaptic transmission by thalidomide. Sample plot of the amplitude of EPSCs as a function of time–thalidomide was added as indicated. (*Inset*) Average synaptic response before (black) and after (red) the addition of thalidomide. (*D*) Summary. (*Left*) Effect of thalidomide on the amplitude of evoked excitatory transmission in m/m and +/+ mice. (*Middle*) Pooled data for all mice; amplitude of evoked EPSCs before (black) and after (red) application of thalidomide. (*Right*) Paired pulse ratio (PPR) before (black) and after (red) the addition of thalidomide.

treatment (Fig. 3*A*) (Wake: dose, F = 28.222, $P < 0.001$; genotype, F = 2.219, $P = 0.122$; interaction dose × genotype, F = 2.317, $P = 0.052$. non-REM sleep: dose, F = 29.612, $P < 0.001$; genotype, F = 1.738, $P = 0.189$; interaction dose × genotype, F = 2.051, $P = 0.081$). Time spent in each vigilance state showed little difference among *Crbn YW/AA* homozygotes, heterozygotes, and wild-type (WT) mice (Fig. 3*B*). EEG delta and theta power during non-REM sleep was not significantly different among the three genotypes (Table 2) (delta power: dose, F = 9.378, $P < 0.001$; genotype, F = 1.492, $P = 0.237$; interaction dose × genotype, F = 0.243, $P = 0.960$. theta power: dose, F = 10.660, $P < 0.001$; genotype, F = 2.523, $P = 0.093$; interaction dose × genotype, F = 0.263, $P = 0.951$). These results indicate that thalidomide similarly induces sleep in *Crbn YW/AA* KI homozygotes and heterozygotes compared with WT littermates.

Excitatory Synaptic Transmission Is Similarly Inhibited in Cortical Slices from *Crbn YW/AA* KI Mice. In acute brain slice preparations in vitro, thalidomide (100 μM) depressed evoked excitatory synaptic transmission in the cortex ($n = 19$; F = 18.015, $P = 0.01$) without a significant interaction between genotype and thalidomide effect (WT, $n = 9$, *Crbn YW/AA*, $n = 10$; F = 0.184, $P = 0.6$)

(Fig. 3 *C* and *D*). The paired-pulse ratio was significantly increased by thalidomide ($n = 19$, F = 6.253, $P = 0.023$), again without a significant interaction between genotype and thalidomide effect (wt, $n = 9$, *Crbn YW/AA*, $n = 10$, F = 3.903, $P > 0.065$) (Fig. 3*D*).

Thalidomide Induces Fos Expression in Vasopressin Neurons of the Supraoptic Nucleus. GABA$_A$ receptor-activating sedatives, such as benzodiazepines, produce hypothalamic Fos staining patterns similar to those observed in sleep (35). Drugs inducing general anesthesia also induce Fos expression in a core set of hypothalamic neurons (34). Anti-Fos immunoreactivity was assessed in brain slices obtained after thalidomide (200 mg/kg i.p.) treatment and compared with vehicle treatment. Unbiased screening of whole-brain serial sections revealed a specific and significant increase in Fos-positive neurons in the supraoptic nuclei (SON) after thalidomide treatment. In addition, Fos expression was significantly reduced in the tuberomammillary nuclei (TMN) (Fig. 4). Furthermore, increased Fos staining was observed in vasopressin-containing, but not oxytocin-containing, SON neurons (Fig. 4 *E–G*).

Hirose et al.

PHARMACOLOGY

Table 2. Power in different frequency bands for increasing doses of thalidomide for WT (m/m), *YW/AA* KI heterozygous (m/+), and *YW/AA* KI homozygous (⁺/⁺) mice

Dose	m/m		m/+		⁺/⁺	
	Delta power, %	Theta power, %	Delta power, %	Theta power, %	Delta power, %	Theta power, %
Vehicle	68.6 ± 2.9	21.5 ± 2.0	65.5 ± 1.3	24.5 ± 1.0	67.9 ± 3.3	22.7 ± 2.4
Thal 100 mg/kg	73.8 ± 3.1	17.7 ± 2.2	72.3 ± 0.8	19.3 ± 0.6	72.2 ± 2.1	19.3 ± 1.5
Thal 200 mg/kg	75.2 ± 2.9	16.8 ± 2.1	73.4 ± 0.9	18.4 ± 0.6	73.1 ± 1.9	18.6 ± 1.4
Thal 400 mg/kg	78.0 ± 2.5	14.7 ± 1.6	75.6 ± 1.1	16.7 ± 0.8	73.6 ± 0.9	18.2 ± 0.6

Delta (1 to 6 Hz) and theta (7 to 11 Hz) power as a percentage of total EEG power (m/m, $n = 4$; m/+, $n = 5$; ⁺/⁺, $n = 4$). Data are mean ± SEM.

Discussion

In the present study, lower doses of thalidomide increased non-REM sleep time without reducing REM sleep time in WT mice. This is consistent with effects reported in other species. For example, thalidomide was found to increase non-REM sleep time and REM sleep time in narcoleptic canines (31) and healthy human volunteers (36). Classical sedatives, acting by increasing GABA$_A$ receptor signaling, produce patterns of Fos labeling in the hypothalamus that resemble those found here under thalidomide (35). Reduced Fos immunoreactivity in the TMN, implying a reduced histaminergic tone, is widely shared among sedatives and found during sleep (35). There were very few previous reports implicating the SON in sleep regulation, although lesions in the SON were observed after severe sleep deprivation (37). Recently, however, increased Fos expression was observed in the SON and para-SON regions after treatment with general anesthetics such as isoflurane, propofol, ketamine, and dexmedetomidine. Furthermore, selective activation of these Fos-positive neurons produced sleep (34). The resemblance of thalidomide-induced Fos expression patterns to those evoked by a number of general anesthetics suggests that thalidomide may activate a common hypothalamic pathway leading to sleep (34). General anesthetics have been found to activate both vasopressin-containing neurons and oxytocin-containing neurons in the SON (34); however, in the present study, thalidomide did not activate oxytocin neurons in the SON. General anesthetics induce analgesia and unresponsiveness when given in sufficient doses. In contrast, thalidomide has no analgesic effect and does not induce unresponsiveness even with high doses (4). The aforementioned difference in hypothalamic Fos activation patterns may reflect the distinct pharmacologic effects of thalidomide and general anesthetics. Indeed, oxytocin has been implicated in pain relief (38, 39).

Sedatives generally shift the excitation-inhibition balance toward inhibition, typically by increasing the function of inhibitory GABA$_A$ receptors (40). Here we observed a shift in the excitation-inhibition balance due to the depression of excitatory synaptic transmission in the cortex; the effect on the paired pulse ratio indicates at least a partially presynaptic effect. Consistent with a previous report, we found no effect of thalidomide on inhibitory synaptic transmission (31). Further efforts to clarify the interaction of thalidomide with the neural circuits that control sleep and waking and its effect on excitatory synaptic transmission are clearly needed.

We show that both mouse FH-CRBN^{WT} and mouse FH-CRBN$^{YW/AA}$ are autoubiquitinated when their specific substrates are absent, suggesting that they form normal Cul4-DDB1-ROC1 E3 ligase complexes (27). Human CRBN$^{YW/AA}$ loses the ability to bind thalidomide while maintaining normal ubiquitin ligase activity (22). We show that thalidomide similarly inhibits autoubiquitination of mouse FH-CRBN^{WT}, but not of mouse FH-CRBN$^{YW/AA}$. This indicates that mouse CRBN$^{YW/AA}$ is indeed no longer sensitive to thalidomide (22), consistent with a previous report on thalidomide-induced inhibition of autoubiquitination

(41). However, thalidomide had an indistinguishable hypnotic effect in *Crbn YW/AA* KI mice compared with WT mice, indicating that no involvement of CRBN-dependent ubiquitination or other CRBN-dependent signaling in thalidomide's hypnotic effect.

In summary, whereas thalidomide no longer affected mouse CRBN$^{YW/AA}$, it had identical hypnotic effects and exerted the same depressant effect on excitatory synaptic transmission in *Crbn YW/AA* KI mice compared with WT mice. Thus, the mechanisms mediating the hypnotic effect of thalidomide do not rely on the CRBN-dependent pathways mediating its teratogenic effect and may involve (i) activation of vasopressin neurons in the SON, which is also observed after application of a wide range of sedatives and anesthetics, and (ii) reduced excitatory synaptic transmission in the cortex. Therefore, it should be possible to develop thalidomide-like hypnotic drugs without thalidomide's teratogenic burden.

Materials and Methods

Reagents. Thalidomide (Wako) is poorly soluble in water. For i.p. administration in vivo, thalidomide was suspended in 0.5% methylcellulose (Wako, Japan). For cell treatment and in vitro electrophysiology, thalidomide was dissolved in dimethyl sulfoxide (DMSO) at 100 mM stock concentration. *N*-ethylmaleimide (Sigma-Aldrich) was dissolved in 100% ethanol at 400 mM immediately before use (22).

Animals. All animal experiments were approved by the Animal Experimental Committee and the Recombinant DNA Experiment Safety Committee at the University of Tsukuba. Animals were housed on a 12:12-h light/dark cycle (with the light automatically turned on at 9:00) at a stable temperature (24.5 ± 0.5 °C), with free access to food and water. Male mice age 10 to 14 wk were used for behavioral experiments, and mice age 21 to 42 d were used for in vitro physiology experiments.

Generation of *Crbn YW/AA* KI Mice. *Crbn* is highly conserved in a variety of species (26); Y384 and W386 residues in human CRBN are homologous to mouse Y387 and W389. A genomic fragment containing the *Crbn* locus was isolated from a C57BL/6 genomic BAC library (Advanced Geno Tech). A targeting vector carrying the *YW/AA* mutation on exon 11 was constructed as shown in Fig. 2*A*. The targeting vector was linearized and electroporated into the C57BL/6N embryonic stem cell line RENKA. Correctly targeted clones were injected into the eight-cell stage ICR mouse embryos, which were cultured to produce blastocysts and later transferred to pseudopregnant ICR females. The resulting male chimeric mice were crossed with female C57BL/6N mice to establish the *Crbn YW/AA-neo* line. To remove the *neo* cassette, *Crbn YW/AA-neo* mice were crossed with *Actb-FLP* KI mice (42).

EEG/EMG Recording and Sleep Analysis. EEG/EMG recordings and sleep/wake analysis were performed as described previously (43). In brief, mice were anesthetized with isoflurane, and EEG/EMG electrodes were implanted and fixed to the skull with dental cement. After >7 d of recovery, mice were moved to recording cages, individually housed in the recording room, and acclimatized to the recording environment for >5 d. The mice were allowed to freely move in the cage while connected to the recording wire. EEG/EMG signals were amplified and filtered (EEG, 0.3 to 300 Hz; EMG, 30 to 300 Hz) using an amplifier AB-611J (Nihon Kohden), then digitized at a sampling rate of 250 Hz and acquired using our SleepyDAC software. States for each 20-s epoch were classified as wakefulness (wake), non-rapid eye movement

www.manaraa.com
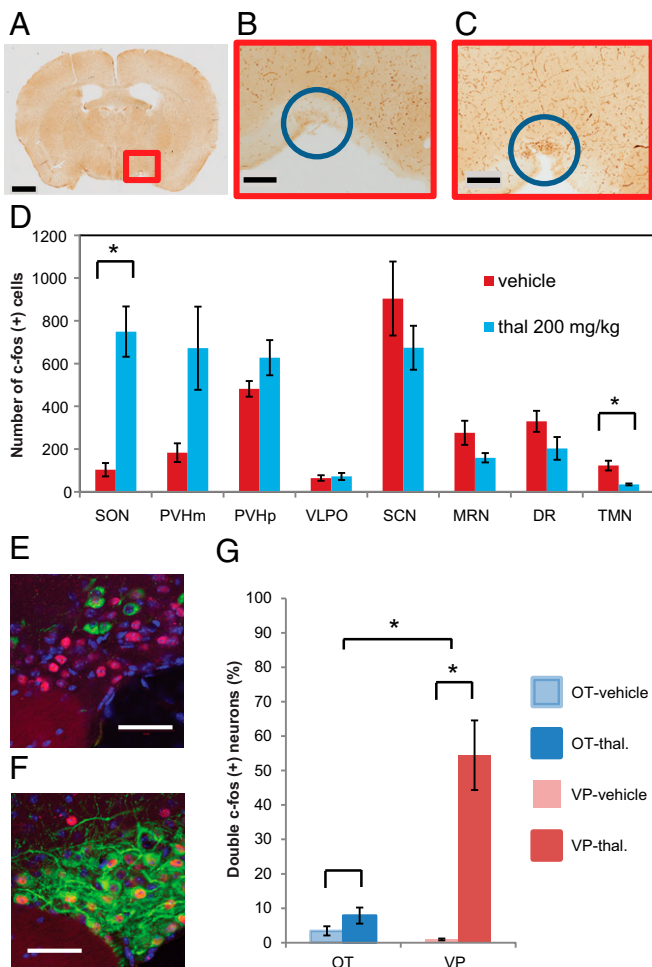
Fig. 4. Effect of thalidomide on hypothalamic FOS expression. Immunostaining against FOS after thalidomide (200 mg/kg i.p.). (*A*) Coronal section of mouse brain with DAB labeling of FOS-expressing neurons. (*B* and *C*) Enlarged area marked in *A* after vehicle treatment (*B*) and after thalidomide treatment (*C*) (Scale bars: 1 mm in *A*; 200 μm in *B* and *C*.) Blue circle marks the supraoptic nucleus. (*D*) Quantification of the effect of thalidomide on FOS expression (mean ± SEM) in different brain regions. Data are mean ± SEM. SON, supraoptic nucleus; PVHm, paraventricular hypothalamic nucleus, magnocellular division; PVHp, paraventricular hypothalamic nucleus, parvicellular division; VLPO, ventrolateral preoptic nucleus; SCN, suprachiasmatic nuclei; MRN, median raphe nucleus; DR, dorsal raphe nucleus; TMN, tuberomammillary nucleus. (*E*) Double immunofluorescence staining in SON against FOS (red) and neurophysin 1 (oxytocin [OT]) (green) (Scale bar: 100 μm.) (*F*) Double-immunofluorescence staining in SON against FOS (red) and copeptin (vasopressin [VP]) (green) (Scale bar: 100 μm.) (*G*) Fraction of FOS-OT and FOS-VP double labeled neurons after vehicle and thalidomide treatment (OT, *n* = 8, T = −1.66, *P* = 0.149; VP, *n* = 8, T = −5.29, *P* = 0.002; unpaired Student's *t* test. Interaction treatment*cell type (OT/VP), *n* = 16, F = 22, *P* = 0.001, two-way ANOVA.

(REM) sleep, or REM sleep, using our SleepyScore software, according to fast Fourier transformation (FFT) and visual inspection.

EEG Spectral Analysis. The power density at each frequency of the EEG signal was calculated as the ratio of the EEG power at each frequency relative to the total EEG power during each state. EEG delta and theta power were determined as the ratio of the integral between 1 to 6 Hz and 7 to 11 Hz EEG power relative to total EEG power, respectively.

Protocols for Thalidomide Treatment. Before the start of EEG/EMG recordings, mice were habituated to i.p. injection by performing two sham injections (one injection per day at ZT12 for 2 consecutive days). We administered the drugs

at dark onset (ZT12). Vehicle and thalidomide suspensions at different concentrations were administered i.p. in a volume of 5 μL/g body weight. EEG/EMG signals during the 24 h following drug application were analyzed. Thalidomide treatments were performed every other day.

Establishing Cell Lines Stably Expressing FLAG-HA–Tagged CRBN (FH-CRBN). We extracted total RNA from the brain of *Crbn YW/AA* KI homozygous and WT mice, and the cDNA was synthesized by RT-PCR (Takara Bio). The sequences of *Crbn* were subcloned into the pcDNA3 0.1(+) vector (Invitrogen), with N-terminal FLAG (DYKDDDDK) and HA (YPYDVPDY) tags inserted by inverse PCR. HEK293A cells were transfected with the pcDNA3.1-FLAG-HA-*Crbn WT* or *YW/AA* using linear polyethyleneimine Max (Polysciences) (44). After G-418 sulfate (Wako) selection, we established cell lines stably expressing FH-CRBN^WT or FH-CRBN^YW/AA.

Biochemical Assessment of Thalidomide's Effects on CRBN. The assay was performed as described previously (22). In brief, cells stably expressing FH-CRBN^WT or FH-CRBN^YW/AA were cultured in DMEM containing FBS (HyClone) and penicillin/streptomycin. We added vehicle or thalidomide at various concentrations to the medium. At 1 h after incubation with thalidomide, we added MG132 (10 μM; Sigma-Aldrich), proteasome inhibitor. After incubation with MG132 for 4 h, cells were lysed in RIPA buffer (20 mM Tris·HCl pH 7.4, 150 mM NaCl, 1 mM EDTA, 1% Triton X-100, and 0.1% SDS) containing 25 μM MG132, 10 mM *N*-ethylmaleimide, and protease inhibitor mixture (ProteoGuard; Takara Bio). Lysates were immunoprecipitated by anti-DYKDDDDK antibody (rabbit; Wako) using DynaBeads Protein G (Thermo Fisher Scientific). The samples were then immunoblotted with anti-HA antibody (rat, 3F10; Roche), or anti-multiubiquitin antibody (mouse, FK2; MBL). Immunoblots from five independent sets of experiments were quantified using the Fusion Solo S imager and Evolution-Capt densitometer software (Vilber-Lourmat), and the effect of thalidomide was statistically examined.

In Vitro Electrophysiology. Mice of either sex were deeply anesthetized with enflurane, and their brains were promptly removed and placed in ice-cold artificial cerebrospinal fluid (ACSF), composed of 124 mM NaCl, 26 mM NaHCO3, 3 mM KCl, 2 mM CaCl, 1 mM MgSO₄, 1.25 mM KH₂PO₄, 10 mM glucose, 300 to 310 mOsm, equilibrated with 95% O₂ and 5% CO₂. The brains were mounted on the stage of a vibrating microtome (Leica VT1200 S) with cyanoacrylate. Coronal sections (250 μm thick) were obtained and allowed to recover in ACSF at room temperature. Slices were submerged in a perfusion chamber placed under an upright microscope (BX51WI; Olympus) fitted with a custom LED IR illumination and Nomarski interference contrast. Slices were superfused with ACSF at a rate of 1 mL/min. Neurons in layers 2/3 and 5/6 of the cortex with a pyramidal cell morphology were patched under visual control. The intracellular solution for current clamp recordings contained 130 mM K gluconate, 1 mM EGTA, 10 mM Hepes, 5 mM MgATP, 0.5 mM NaGTP, and 5 mM NaCl. The pH was adjusted to 7.3 with KOH and osmolarity to 290 to 300 mOsm. The intracellular solution for voltage-clamp recordings contained 130 mM Cs gluconate, 1 mM EGTA, 10 mM Hepes, 5 mM MgATP, 0.5 mM NaGTP, and 5 mM NaCl. The pH was adjusted to 7.33 with CsOH and osmolarity to was 285 to 300 mOsm. Borosilicate patch pipettes were pulled to an open-tip resistance of 2 to 4 MΩ. Signals were amplified (Axopatch 700A; Molecular Devices) and then digitized using customized routines in commercial software (IGOR Pro; WaveMetrics). Evoked synaptic responses were produced through extracellular stimulation with monopolar glass pipette electrodes filled with ACSF. Spontaneous events were detected post hoc (Mini Analysis Software; Synaptosoft). Excitatory synaptic currents were measured at holding potentials of −60 mV for evoked events and −70 mV for spontaneous events; inhibitory synaptic currents were measured at a 0-mV holding potential.

Thalidomide-Induced Fos Expression. Mice were treated with a 200 mg/kg dose of thalidomide or vehicle at dark onset (ZT12). At 2 h after treatment, mice were anesthetized with isoflurane and transcardially perfused with 4% paraformaldehyde and 0.1 M phosphate buffer (PB), pH 7.4 (4% PFA). Dissected brains were fixed overnight in 4% PFA at 4 °C. Brains were sectioned into 40-μm-thick coronal sections with a vibratome (VT1000S; Leica) and harvested every three sections. Brain sections were washed three times in 0.1 M PB, 0.5% BSA, and 0.25% Triton X-100 (blocking solution). Sections were treated with rabbit anti-FOS antibody (1:10,000, Merck Millipore) overnight at 4 °C. Sections were washed three times in blocking solution and incubated in biotinylated goat anti-rabbit IgG antibody (1:1,000; Vector Labs) for 2 h. Sections were treated with the VECTASTAIN ABC Elite Kit (Vector Labs) and the DAB Peroxidase HRP Substrate Kit (Vector Labs). Sections were then mounted onto MAS-coated glass slides (Matsunami), coverslipped, dehydrated

Hirose et al.

www.manaraa.com

PHARMACOLOGY

in alcohol, cleared in xylene, and scanned with a NanoZoomer digital slide scanner (Hamamatsu) and an Axio Imager microscope (Carl Zeiss).

Double Immunostaining. Brain sections were prepared as described above. Sections were incubated overnight at 4 °C in rabbit anti-Fos antibody (1:10,000), goat anti-copeptin (biomarker of vasopressin) antibody (1:400, Santa Cruz Biotechnology), or goat anti-neurophysin 1 (biomarker of oxytocin) antibody (1:400, Santa Cruz Biotechnology). Sections were washed three times in blocking solution and then incubated with Alexa Fluor 594 chick anti-rabbit IgG antibody (1:1,000; Thermo Fisher Scientific) and Alexa Fluor 488 donkey anti-goat IgG antibody (1:1,000; Thermo Fisher Scientific). Confocal laser scanning was performed with an LSM700 laser scanning confocal microscope (Carl Zeiss).

Statistical Analysis. Statistical analyses were done using SPSS software (IBM). The behavioral data for C57BL/6N mice were analyzed using one-way ANOVA. The data comparing WT and *Crbn YW/AA* KI mice were analyzed using two-way ANOVA. Data on synaptic transmission were analyzed using the paired Student *t* test. The effect of thalidomide on the number of cells expressing FOS was analyzed using the unpaired Student *t* test. The effect of

thalidomide on CRBN autoubiquitination was analyzed using one-way repeated-measures ANOVA with Mauchly's test of sphericity, followed by the Bonferroni-corrected post hoc paired Student's *t* test when appropriate. The fractions of oxytocin and vasopressin in FOS double-positive neurons were assessed using two-way ANOVA.

Data Availability. All study data are included in the main text.

1. J. K. Walsh *et al.*, Nighttime insomnia symptoms and perceived health in the America Insomnia Survey (AIS). *Sleep* **34**, 997–1011 (2011).
2. S. Stranges, W. Tigbe, F. X. Gómez-Olivé, M. Thorogood, N. B. Kandala, Sleep problems: An emerging global epidemic? Findings from the INDEPTH WHO-SAGE study among more than 40,000 older adults from 8 countries across Africa and Asia. *Sleep* **35**, 1173–1181 (2012).
3. T. L. Schwartz, V. Goradia, Managing insomnia: An overview of insomnia and pharmacologic treatment strategies in use and on the horizon. *Drugs Context* 2013, 212257 (2013).
4. G. F. Somers, Pharmacological properties of thalidomide (alpha-phthalimido glutarimide), a new sedative hypnotic drug. *Br. J. Pharmacol. Chemother.* **15**, 111–116 (1960).
5. H. B. Taussig, A study of the German outbreak of phocomelia. The thalidomide syndrome. *JAMA* **180**, 1106–1114 (1962).
6. I. M. Leck, E. L. Millar, Incidence of malformations since the introduction of thalidomide. *BMJ* **2**, 16–20 (1962).
7. W. Lenz, K. Knapp, Thalidomide embryopathy. *Arch. Environ. Health* **5**, 100–105 (1962).
8. A. E. Rodin, L. A. Koller, J. D. Taylor, Association of thalidomide (Kevadon) with congenital anomalies. *Can. Med. Assoc. J.* **86**, 744–746 (1962).
9. A. L. Speirs, Thalidomide and congenital abnormalities. *Lancet* **1**, 303–305 (1962).
10. G. S. Somers, Thalidomide and congenital abnormalities. *Lancet* **1**, 912–913 (1962).
11. I. D. Fratta, E. B. Sigg, K. Maiorana, Teratogenic effects of thalidomide in rabbits, rats, hamsters, and mice. *Toxicol. Appl. Pharmacol.* **7**, 268–286 (1965).
12. J. G. Wilson, R. Fradkin, Teratogeny in nonhuman primates, with notes on breeding procedures in Macaca mulatta. *Ann. N. Y. Acad. Sci.* **162**, 267–277 (1969).
13. L. Levy, P. Fasal, N. E. Levan, R. I. Freedman, Treatment of erythema nodosum leprosum with thalidomide. *Lancet* **2**, 324–325 (1973).
14. S. Makonkawkeyoon, R. N. Limson-Pobre, A. L. Moreira, V. Schauf, G. Kaplan, Thalidomide inhibits the replication of human immunodeficiency virus type 1. *Proc. Natl. Acad. Sci. U.S.A.* **90**, 5974–5978 (1993).
15. W. A. Hanekom *et al.*, The immunomodulatory effects of thalidomide on human immunodeficiency virus-infected children. *J. Infect. Dis.* **184**, 1192–1196 (2001).
16. R. J. D'Amato, M. S. Loughnan, E. Flynn, J. Folkman, Thalidomide is an inhibitor of angiogenesis. *Proc. Natl. Acad. Sci. U.S.A.* **91**, 4082–4085 (1994).
17. A. L. Moreira *et al.*, Thalidomide exerts its inhibitory action on tumor necrosis factor alpha by enhancing mRNA degradation. *J. Exp. Med.* **177**, 1675–1680 (1993).
18. L. G. Corral, G. Kaplan, Immunomodulation by thalidomide and thalidomide analogues. *Ann. Rheum. Dis.* **58** (suppl. 1), I107–I113 (1999).
19. M. Larkin, Low-dose thalidomide seems to be effective in multiple myeloma. *Lancet* **354**, 925 (1999).
20. S. Singhal *et al.*, Antitumor activity of thalidomide in refractory multiple myeloma. *N. Engl. J. Med.* **341**, 1565–1571 (1999).
21. J. B. Bartlett, K. Dredge, A. G. Dalgleish, The evolution of thalidomide and its IMiD derivatives as anticancer agents. *Nat. Rev. Cancer* **4**, 314–322 (2004).
22. T. Ito *et al.*, Identification of a primary target of thalidomide teratogenicity. *Science* **327**, 1345–1350 (2010).
23. J. Krönke *et al.*, Lenalidomide causes selective degradation of IKZF1 and IKZF3 in multiple myeloma cells. *Science* **343**, 301–305 (2014).

24. G. Lu *et al.*, The myeloma drug lenalidomide promotes the cereblon-dependent destruction of Ikaros proteins. *Science* **343**, 305–309 (2014).
25. J. Krönke *et al.*, Lenalidomide induces ubiquitination and degradation of CK1α in del(5q) MDS. *Nature* **523**, 183–188 (2015).
26. J. J. Higgins, J. Pucilowska, R. Q. Lombardi, J. P. Rooney, A mutation in a novel ATP-dependent Lon protease gene in a kindred with mild mental retardation. *Neurology* **63**, 1927–1931 (2004).
27. A. A. Akuffo *et al.*, Ligand-mediated protein degradation reveals functional conservation among sequence variants of the CUL4-type E3 ligase substrate receptor cereblon. *J. Biol. Chem.* **293**, 6187–6200 (2018).
28. J. Lu *et al.*, Hijacking the E3 ubiquitin ligase cereblon to efficiently target BRD4. *Chem. Biol.* **22**, 755–763 (2015).
29. N. Sawamura *et al.*, The neuroprotective effect of thalidomide against ischemia through the cereblon-mediated repression of AMPK activity. *Sci. Rep.* **8**, 2459 (2018).
30. T. Y. Choi *et al.*, BK channel blocker paxilline attenuates thalidomide-caused synaptic and cognitive dysfunctions in mice. *Sci. Rep.* **8**, 17653 (2018).
31. T. Kanbayashi *et al.*, Thalidomide, a hypnotic with immune modulating properties, increases cataplexy in canine narcolepsy. *Neuroreport* **7**, 1881–1886 (1996).
32. N. Stavropoulos, M. W. Young, Insomniac and Cullin-3 regulate sleep and wakefulness in Drosophila. *Neuron* **72**, 964–976 (2011).
33. C. Pfeiffenberger, R. Allada, Cul3 and the BTB adaptor insomniac are key regulators of sleep homeostasis and a dopamine arousal pathway in Drosophila. *PLoS Genet.* **8**, e1003003 (2012).
34. L.-F. Jiang-Xie *et al.*, A common neuroendocrine substrate for diverse general anesthetics and sleep. *Neuron* **102**, 1053–1065.e4 (2019).
35. J. Lu *et al.*, Role of endogenous sleep-wake and analgesic systems in anesthesia. *J. Comp. Neurol.* **508**, 648–662 (2008).
36. T. Kanbayashi *et al.*, Thalidomide increases both REM and stage 3-4 sleep in human adults: A preliminary study. *Sleep* **22**, 113–115 (1999).
37. M. M. Eiland *et al.*, Increases in amino-cupric-silver staining of the supraoptic nucleus after sleep deprivation. *Brain Res.* **945**, 1–8 (2002).
38. Q. Xin, B. Bai, W. Liu, The analgesic effects of oxytocin in the peripheral and central nervous system. *Neurochem. Int.* **103**, 57–64 (2017).
39. Y. Meguro *et al.*, Neuropeptide oxytocin enhances μ opioid receptor signaling as a positive allosteric modulator. *J. Pharmacol. Sci.* **137**, 67–75 (2018).
40. T. B. Sloan, Anesthetic effects on electrophysiologic recordings. *J. Clin. Neurophysiol.* **15**, 217–226 (1998).
41. Y. Liu *et al.*, A novel effect of thalidomide and its analogs: Suppression of cereblon ubiquitination enhances ubiquitin ligase function. *FASEB J.* **29**, 4829–4839 (2015).
42. J. Kono *et al.*, Distribution of corticotropin-releasing factor neurons in the mouse brain: A study using corticotropin-releasing factor-modified yellow fluorescent protein knock-in mouse. *Brain Struct. Funct.* **222**, 1705–1732 (2017).
43. R. M. Chemelli *et al.*, Narcolepsy in orexin knockout mice: Molecular genetics of sleep regulation. *Cell* **98**, 437–451 (1999).
44. S. E. Reed, E. M. Staley, J. P. Mayginnes, D. J. Pintel, G. E. Tullis, Transfection of mammalian cells using linear polyethylenimine is a simple and effective means of producing recombinant adeno-associated virus vectors. *J. Virol. Methods* **138**, 85–98 (2006).

www.manaraa.com